Applied Mechanics and Materials
ISSN: 1662-7482, Vol. 885, pp 64-74
doi:10.4028/www.scientific.net/AMM.885.64

Submitted: 2018-04-16
Revised: 2018-07-26
Accepted: 2018-07-27
Online: 2018-11-20

Numerical Comparison of Three Different Feedback Control Schemes Applied on a Forming Operation

B. Endelt[1,a]

Department of Materials and Production, Fibigerstræde 16, Aalborg University, Denmark

[a]endelt@pm.aau.dk

Keywords: Metal forming, process control, feedback control, iterative learning control, non-linear least square

Abstract. Feedback and process control of metal forming processes has received increasing attention the last decade. Basically there exist four control philosophies; control of process parameters during the punch stroke, iterative learning control (based on historical data), a combination iterative learning and feedback control and finally feed-forward control. The present work will present three different control schemes which all are based on feedback philosophy i.e. control during the punch stroke or iterative learning control, where process parameters are updated according to process history. The three control schemes are tested using a non-linear finite element model of a square deep-drawing and finally pros and cons are discussed based on the numerical results.

Introduction

It is generally accepted that the deep drawing and stamping operations are non-static over time i.e. changes in the material parameters, friction and lubrication, tool and press deflection, etc. all influence the process stability. The process noise can generally be divided into two categories:

- **Non-repetitive uncertainties** - variance in sheet thickness and uneven lubrication.
- **Repetitive uncertainties** - changes in the material properties, tool wear and tool temperature.

The non-repetitive uncertainties can be categorised as normal distributed noise without any trends or development over time and are generally handled through an open loop strategy where the stability is enforced by conservative and robust tool-designs.

The repetitive uncertainties can result in process breakdown and typically requires manual process adjustment e.g. adjustment of the blank-holder force, lubrication, shimming etc.

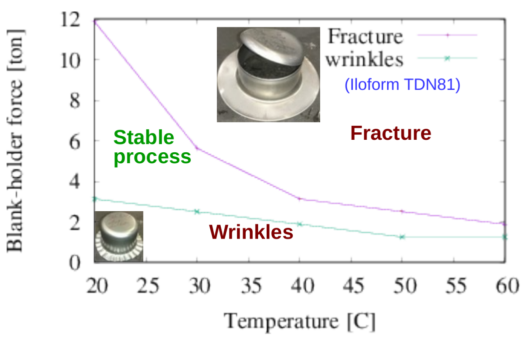

(a) The influence of tool temperature on the process window for a cylindrical deep drawing.

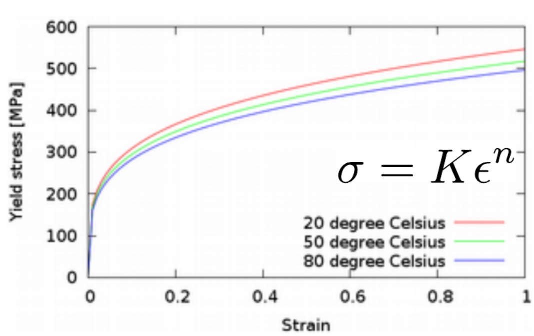

(b) Tensile test of DC06 at room temperature and elevated temperature, the strain hardening is modelled using a Hollomon Swift model.

Fig. 1: Temperature dependent process window and hardening curve.

Due to plastic work the tool temperature will increase during the first half hour production, the steady state temperature is typical in the range of 60-80°C [1, 7]. Figure 1 shows the limiting blank-holder force for a cylindrical deep drawing for different tool temperatures, in this case the process window (defined as range between the upper and lower blank-holder force) is reduced from 9 ton at room temperature to less than 1 ton for a tool temperature of 60°C. The correlation between tool temperature and process stability is very complex, however it is safe to conclude that tool temperature will influence friction conditions as well as material properties, see figure 1.

This paper will present three different approaches to feedback control of stamping and deep drawing operation. Many, different approaches has been proposed in the literature, however, they can all be divided into four categories, see figure 2

- **Feedback control:** Corrective actions are taken during the punch stroke e.g. controlling the blank-holder force [5].
- **Feedback control and Iterative learning control:** A combination of in-process feedback control (corrections during the punch stroke) and an iterative learning control system which transfer process information from part to part [3, 1]
- **Iterative learning control:** A system which update process parameters based on post-process data - where the control system transfers information from part to part [4, 2].
- **Feed-forward (control):** The process parameters are estimated based on material parameters see e.g [6], tool temperature, sheet thickness, etc.

Feedback control is based on the ability to sample data from the process and one of the key elements in feedback control is the ability to establish a unique relation between the sampled output and input parameters (process parameters).

We are dealing with plastic deformation and it seems reasonable to chose an output signal $y(k)$ which reflects plastic deformation. Both material flow into the die cavity [8] and flange draw-in [10] has been proposed in the literature. The first two control algorithms (feedback control and the combined feedback and ILC)are based on the flange draw-in sampled during the punch stroke [5, 3, 1]. The last ILC algorithm is only using the final flange geometry as input, thus data can be sampled after the tool is opened using e.g laser scanners or image processing. [4, 2].

Numerical example

Deep-drawing of a square part enables full control of the flange draw-in using a special designed shimming system, where the blank-holder is locally deformed using hydraulic pressure. The deflection of the blank-holder is controlled by four cavities located on each side of the square cup, giving a total of five process parameters, including the blank-holder force, which can be individual adjusted, see figure 4.

The performance of the three different control schemes is evaluated using a blank material with an uneven thickness distribution (0.95 to 1.05mm left to right) and changes in the material parameters, see figure 3b. The new material batch will result in uneven flange draw-in and process instability, see figure 7c. A well performing algorithm should stabilise the process by reproducing the reference flange geometry and the reference thickness distribution, see figure 3a.

Modelling the control system

Lim et al. [7] reviewed advances in feedback control of sheet metal forming processes and concluded that one of the requirement for designing and developing in-process-controllers are accurate models of the forming process.

The current control schemes are all designed using a finite element model of the stamping or deep drawing process. Where feedback gain factors (two first control systems) are identified solving a non-linear optimal control problem where the system is modelled using LS-Dyna and the non-linear

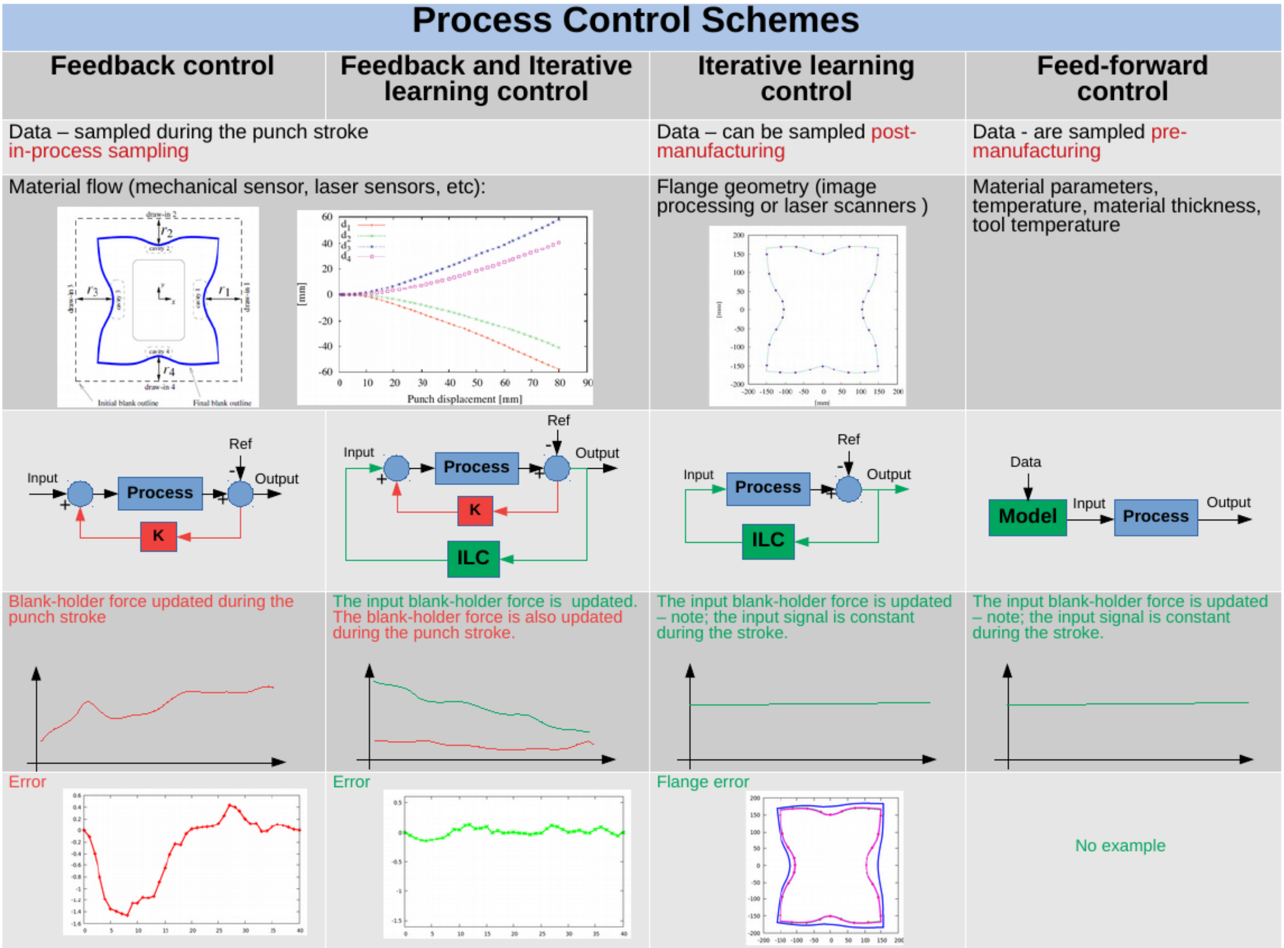

Fig. 2: Four different process control schemes with different level of control and different demands regarding sampling technologies. Where the red loop indicates in-process control and the green loop is pre- or post-processing control.

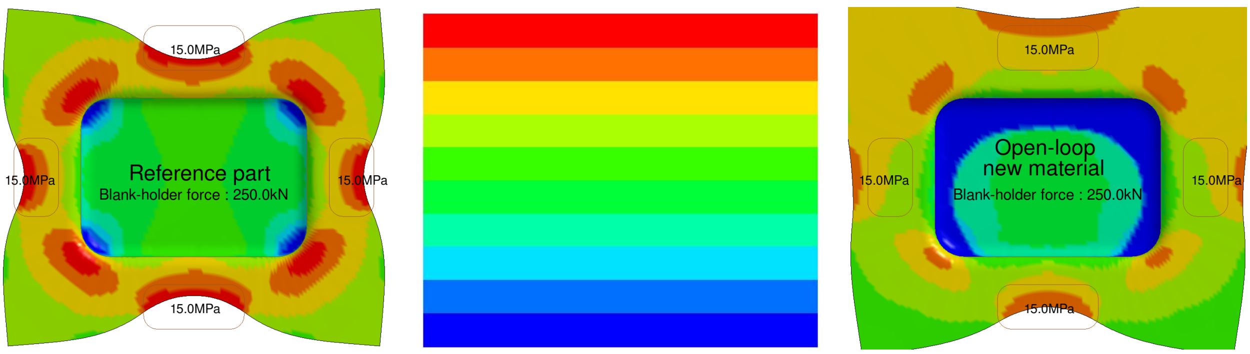

(a) Reference stable process - thickness range 0.68-1.16mm using an initial blank thickness of 1mm and material parameters: K=550MPa and n=0.25

(b) New material batch, initial thickness range 0.95-1.05mm, Material parameters K=450 and n=0.23

(c) Process outcome; using new parameters K=450MPa and n=0.23 and an uneven thickness distribution mm (0.95 to 1.05mm left to right). The process is unstable with a final thickness range 0.26-1.21mm

Fig. 3: Process parameters; using an equal cavity pressures was 15MPa and blank-holder force 250kN.

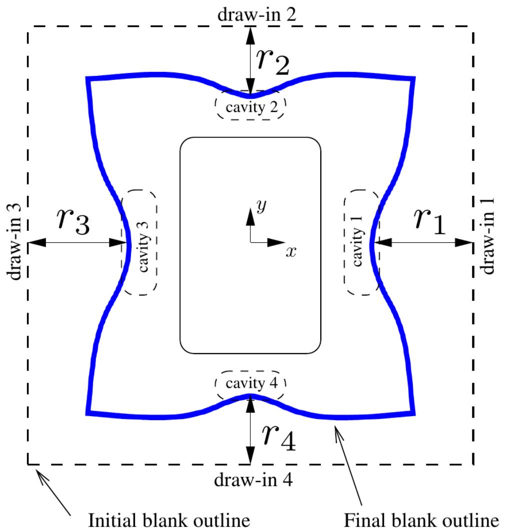

(a) Draw-in measurements and the location of the cavities.

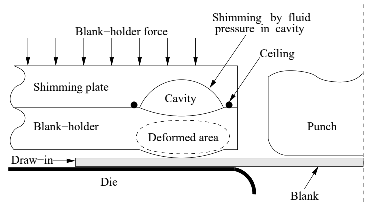

(b) Schematic illustration of the shimming system enabling local control of the flange draw-in.

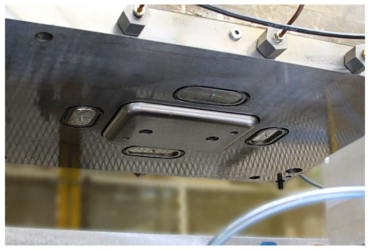

(c) Experimental setup.

Fig. 4: Process parameters (cavities and blank-holder force) and location of the draw-in sample points.

optimal control problem is solved iterative using a non-linear least square solver. The third ILC algorithm is also based on a non-linear least square formulation where the Jacobian matrix is calculated via the finite element model. It is important to note that the finite element model is only used during the design phase and are not involved in an experimental set-up.

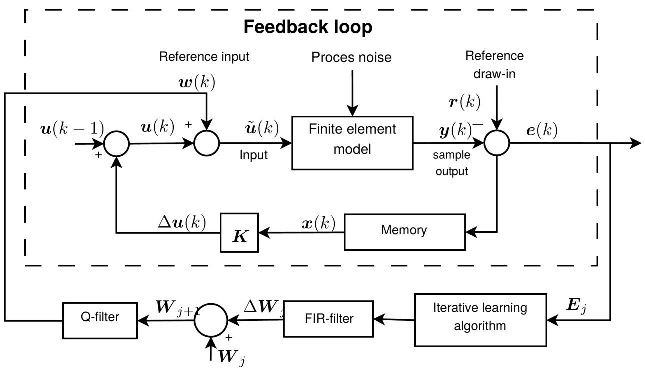

Fig. 5: Illustration of the two control loops. Where the feedback loop, controls the error development during the punch stroke. The outer iterative learning loop transfers information from part to part [1].

Feedback Control

One approach to reduce the scrap rate is introducing an in-process feedback control. Polyblank et.al gives an extensive review of the area covering more than two decades of research activities, within the field of feedback control applied on various metal-forming processes [9]. In the current paper the plant (model of the control system) is based on a finite element model and the feedback constants (gain factors) are identified solving a non-linear optimal control problem.

$$f(\boldsymbol{K}) = \frac{1}{2}\sum_{k=1}^{m} \boldsymbol{e}_k^T \boldsymbol{Q}_1 \boldsymbol{e}_k + \frac{1}{2}\sum_{k=1}^{m} \Delta\boldsymbol{u}_k^T \boldsymbol{Q}_2 \Delta\boldsymbol{u}_k \quad (1)$$

The weighing coefficients $\boldsymbol{Q}_1$ and $\boldsymbol{Q}_2$ are used to control the stability of the system, where $\boldsymbol{Q}_1 = q_1\boldsymbol{I}$ controls the impact of the draw-in error and $\boldsymbol{Q}_2 = q_2\boldsymbol{I}$ can be interpreted as a damping factor.

Feedback during the punch stroke

The in-process feedback loop, modelling and solution strategy has been developed over a series of articles, see [5]. The control scheme is based on the notion that time series can be used to predict the state of a system one step ahead, x_{j+1}, is estimated by assuming a linear correlation between the current and previous samples. If you can predict the state of the system one step ahead, then this information can also be used to take corrective actions thus, the state vector can be defined as:

$$\boldsymbol{x}^T(k) = [\underbrace{\tilde{e}_1(k)\ \tilde{e}_1(k-1)}_{\text{Sample point 1}}\ \ldots\ \underbrace{e^a(k)\ \ e^a(k-1)}_{\text{average draw-in}}]$$

The updated system input $\tilde{u}(k)$ is then defined as

$$\tilde{\boldsymbol{u}}(k) = \boldsymbol{w}(k) + \boldsymbol{u}(k) \tag{2}$$

where $\boldsymbol{w}(k)$ represents the reference blank-holder force and cavity pressure and $u(k)$ represents the controller input, defined as:

$$\boldsymbol{u}(k) = \boldsymbol{u}(k-1) + \Delta\boldsymbol{u}(k) \tag{3}$$

where the controller effort $\Delta\boldsymbol{u}(k)$ was calculated according to

$$\Delta\boldsymbol{u}(k) = \boldsymbol{K}\boldsymbol{x}(k) \tag{4}$$

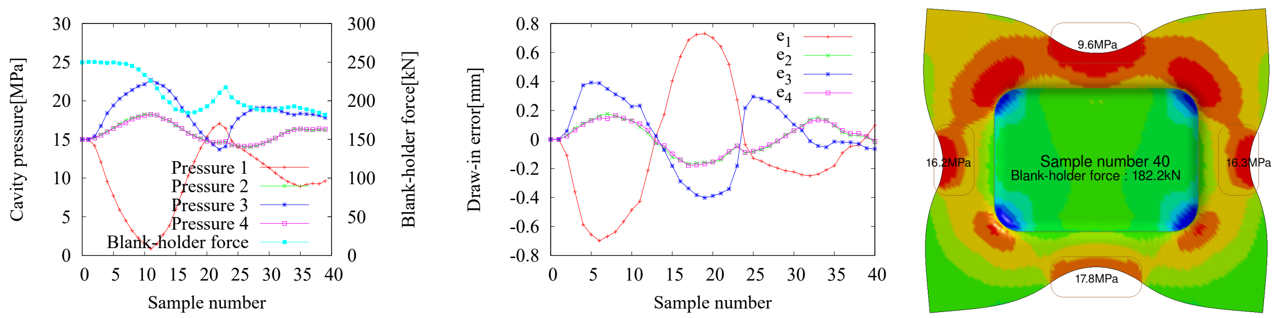

(a) Process parameters using the feedback loop (b) Least square flange draw-in error in mm (c) Thickness for the final part - range 0.67-1.2mm

Fig. 6: Feedback (during the punch stroke) process variables i.e. the first part produced after changing the material properties. Note the flange position is sampled as a function of punch displacement (total punch displacement 80mm) with a interval of 2mm i.e. a total of 40 samples during the punch stroke.

The control system eliminates the draw-in error during the punch stroke by adjusting both the cavity pressure and the blank-holder force. Figure 6b shows the draw-in error converges to zero during the punch stroke. However, some oscillation in the draw-in error and input parameters can be observed. The process instability, figure 7c, is eliminated and the thickness distribution in the final part is in the range of 0.67-1.2mm, see figure 11d.

Feedback and Iterative Learning Control

The in-process control system do not take in account that stamping and deep-drawing processes are repetitive processes running over a limited time span (process time in the range of 2-3 seconds) i.e. if the process is subject to a repetitive uncertainty (e.g. a new material batch) then the in-process control system will receptively correct the same error part after part. As a result, the repetitive uncertainties, will eventually use all the available correctable bandwidth i.e. the in-process control system will be unable to compensate for non-repetitive uncertainties. This problem is addressed by introducing a second control loop, which take advantage of the repetitive process layout and updates the process parameters based on historical data i.e. data from the previously produced part is used to update the input $\boldsymbol{w}(k)$, see figure 5.

A linear learning algorithm is generally preferred and taking the form:

$$\boldsymbol{W}_{j+1} = \boldsymbol{W}_j + \underbrace{\boldsymbol{G}\boldsymbol{E}_j}_{\Delta \boldsymbol{W}_j} \tag{5}$$

where j represents the ILC iteration index, $\boldsymbol{E}_j$ and $\boldsymbol{W}_j$ are $m \times n$ matrices representing the current error and reference input.

The gain matrix $\boldsymbol{G}$ is a $m \times m$ lower triangular matrix, with ϕ_1 in the diagonal and $\phi_1 + \phi_2$ below the diagonal:

$$\boldsymbol{G} = \begin{bmatrix} \phi_1 & 0 & \dots & 0 & 0 \\ \phi_1 + \phi_2 & \phi_1 & \dots & 0 & 0 \\ \vdots & \vdots & \ddots & \vdots & \vdots \\ \phi_1 + \phi_2 & \phi_1 + \phi_2 & \phi_1 + \phi_2 & \phi_1 & 0 \\ \phi_1 + \phi_2 & \phi_1 + \phi_2 & \phi_1 + \phi_2 & \phi_1 + \phi_2 & \phi_1 \end{bmatrix}$$

If a new material batch is taken into production, the feedback loop will initially try to minimise the error during the manufacturing of the first part - then the ILC algorithm will gradually take over reducing the error by adjusting the process parameters corresponding to the new operational conditions. By adjusting the reference input $\boldsymbol{w}(k)$ trajectory, see figure 9. The draw-in error, during the punch stroke, is almost eliminated for 20th part following the change in the material parameters. The main properties of the control system, combining feedback and iterative learning control can be summarised as:

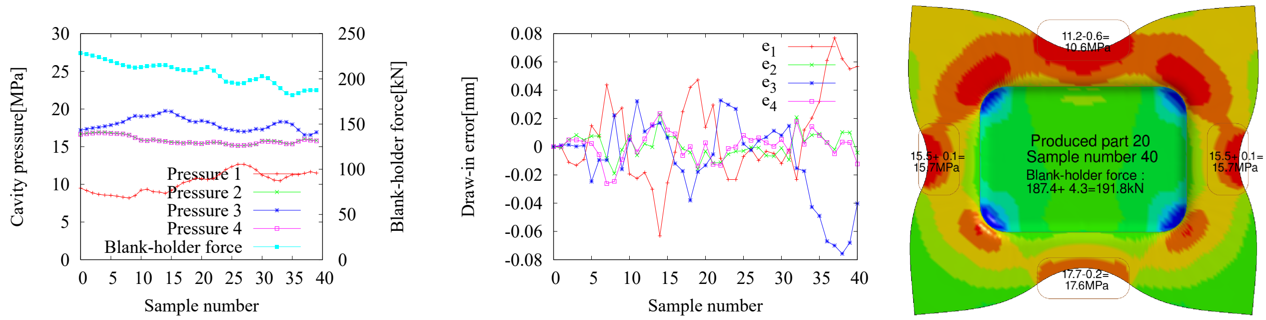

(a) Process parameters applied for part number 20

(b) Draw-in error for iteration 20.

(c) Combined feedback and ILC thickness distribution after 20 iteration - thickness range 0.67-1.19mm.

Fig. 7: Process variables plotted for iteration 20 i.e. part number 20 produced after the change in material properties.

- **Advantage:** The algorithm offers full control over the reference input trajectory $\boldsymbol{w}(k)$ i.e. variable blank-holder and cavity pressures can be prescribed as a function of the punch displacement, see figure 7a.

- **Disadvantage:** Accurate and robust draw-in samples are required as a sensor fallout will result in process instability. This is one of the main limitations preventing industrial applications.

Iterative Learning Control

Endelt and Volk [4] identified two major obstacles which need to be addressed before an industrial implementation is possible:

- The proposed control algorithms are often limited by the ability to sample process data with both sufficient accuracy and robustness - this lack of robust sampling technologies is one of the main barriers preventing successful industrial implementation.
- Limitation in the current press designs; many of the presses currently used in industry only offer limited opportunities to change the blank-holder force during the punch stroke. Even if, the press offers the opportunity to change the blank-holder force the reaction speed may be insufficient compared with the production rate in an industrial application.

Choose the ”optimal” process parameters x^* and the step size scalar α and s_{max}, load or sample the reference flange geometry $\boldsymbol{y}^{ref}$. Initialize the counter $k = 1$, k_{max} and set $\boldsymbol{x}_k = \boldsymbol{x}^*$.
Load the Jacobian matrix $\boldsymbol{J}(\boldsymbol{x}^*)$ and calculate the Hessian matrix using the Gauss-Newton approximation $\boldsymbol{H}^* \approx \boldsymbol{J}(\boldsymbol{x}^*)^T \boldsymbol{J}(\boldsymbol{x}^*)$
while $(k < k_{max})$ **do**
    Update the flange geometry $\boldsymbol{y}_k$, the residual vector and the gradient according to:
    Residual vector: $\boldsymbol{r}_k = \boldsymbol{y}_k - \boldsymbol{y}^{ref}$
    Gradient: $\nabla f(\boldsymbol{x}_k) = \boldsymbol{J}(\boldsymbol{x}^*)^T \boldsymbol{r}(\boldsymbol{x}_k)$
    $\boldsymbol{d}_k = -\frac{\nabla f(\boldsymbol{x}_k)}{\boldsymbol{H}^*}$
    Calculating maximum step size according to:
    if $(s_{max} > 0)$ **then**
        $\alpha_{max} = \min\left(\alpha, \frac{s_{max}}{\max(\max(\boldsymbol{d}_k), -\min(\boldsymbol{d}_k))}\right)$
    else
        $\alpha_{max} = \alpha$
    end if
    Update the process parameters $\boldsymbol{x}_{k+1}$ according to:
    $\boldsymbol{x}_{k+1} = \boldsymbol{x}_k - \alpha_{max} \frac{\nabla f(\boldsymbol{x}_k)}{\boldsymbol{H}^*}$
    $k = k + 1$
end while
End

Fig. 8: Flange fitting iterative learning control algorithm based on a non-linear least square formulation. The Jacobian matrix is approximated using finite difference and it is only calculated for the reference point $\boldsymbol{x}^*$. The following parameters were used $\alpha = 0.5$ and $s_{max} = 100$kN [2].

The third algorithm is based on a classical Gauss-Newton formulation where the control problem is treated as non-linear curve fitting problem. Where the objective is to minimise the least square error between a reference flange geometry $\hat{y}$ and the current flange geometry y. The ”optimal” or reference flange geometry which represents the stable process were represented by 32 sample points which were collected along the flange edge, see figure 9a.

The non-linear optimization algorithm, can be reformulated to an iterative learning control scheme. If the flange fitting problem is assumed to be convex and close to linear, in a sufficient region surrounding the optimal process parameters $\boldsymbol{x}^*$ which also defines the optimal flange geometry. Under these assumptions, it is only necessary to calculate the Jacobian representation at the point $\boldsymbol{x}^*$. Thus, only one Jacobian matrix is defined $\boldsymbol{J}(\boldsymbol{x}^*)$, which will govern the optimization problem, for any set of parameters $\boldsymbol{x}_k$ and any residual vector $\boldsymbol{r}_k$ which are sufficient close to $\boldsymbol{x}^*$.

The Jacobian is a $m \times n$ matrix, where n represents in this case represents the number of process parameters $\boldsymbol{x}$ and m represents the number of sample points $\boldsymbol{y}$. The j-th column of the Jacobian matrix gives the sensitivity of the flange draw-in error $\boldsymbol{r}$ with respect to the process parameter x_j. The vectors $\partial \boldsymbol{r}/\partial x_j$ represents the sensitivity of each sample point i with respect to process parameters x_j, the algorithm is summarised in figure 8.

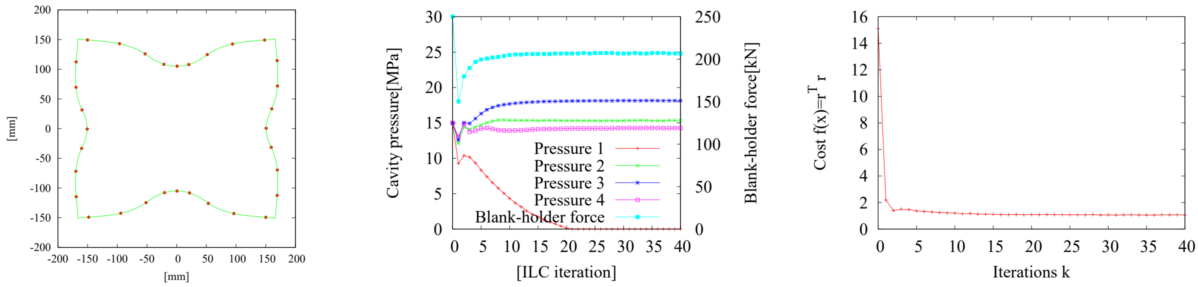

(a) Reference edge - represented by 32 samples.

(b) Process parameters as a function of ILC iteration.

(c) Least square flange draw-in error

Fig. 9: Process variables and least square error as a function of ILC iterations.

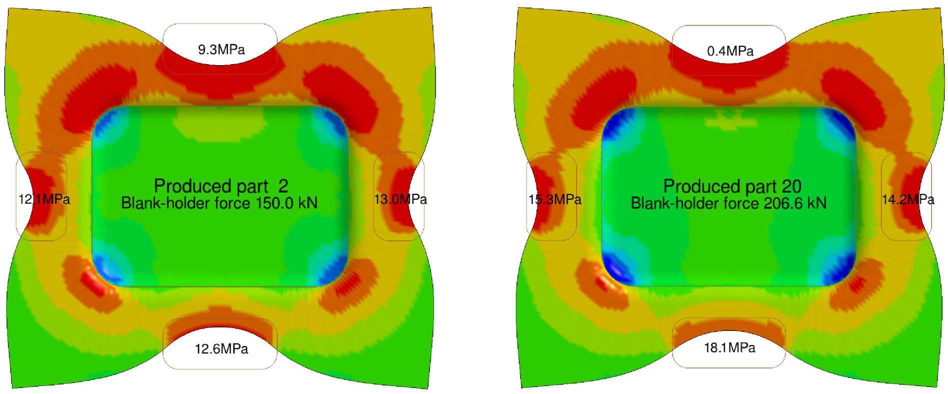

(a) Thickness distribution for the second part following the shift, thickness range 0.72-1.22mm

(b) Part number 20 following the shift, thickness range 0.67-1.19mm

Fig. 10: Thickness distribution for the second and 20th part following the shift in material properties.

The ILC algorithm (based on post process data) stabilises the process within 5-10 produced parts, see figure 9. Figure 10 shows the thickness distribution for the second and 20th part produced after the change in material properties, note the close resembles between the two components, this indicates that only the first part produced, following the shift, will be non conforming, see figure 7c.

Conclusions

All three control schemes stabilised the process and producing parts with almost identical thickness distributions, see figure 11. Furthermore, figure 12 shows the flange geometry produced by the three control schemes, they all produce a flange geometry which are very close to the reference part.

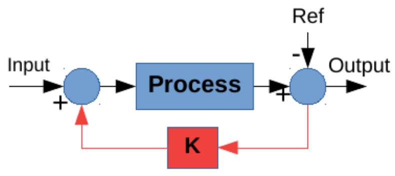

(a) Feedback system controlling process parameters during the punch stroke.

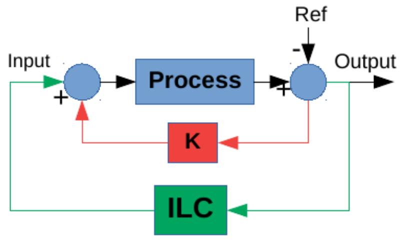

(b) Feedback and ILC loop.

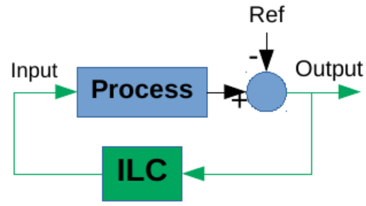

(c) ILC control loop.

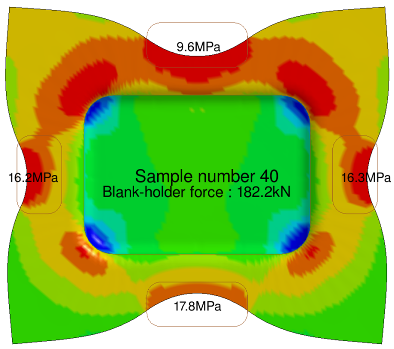

(d) Feedback system - Thickness for the final part - range 0.67-1.2mm

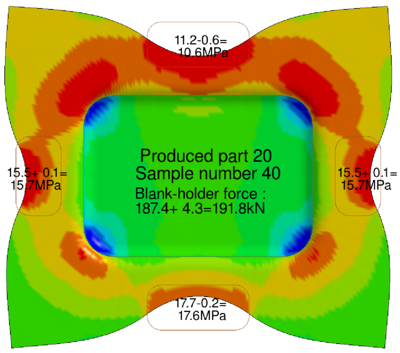

(e) Combined system (feedback and ILC) thickness distribution after 20 iteration - thickness range 0.67-1.19mm

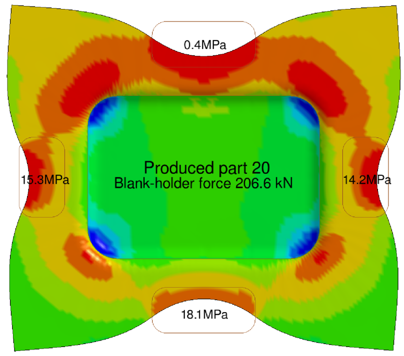

(f) ILC system - Part number 20 following the shift, thickness range 0.67-1.19mm

Fig. 11: Comparison of the three control schemes

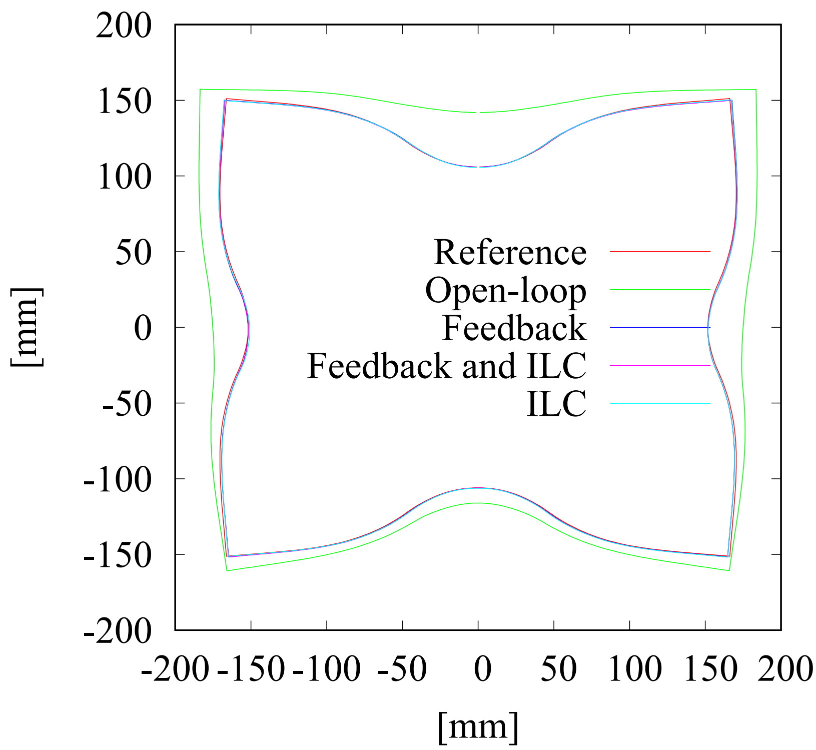

Fig. 12: Reference flange geometry plotted against the flange geometry produced by the different control schemes.

- **Feedback:** The feedback system is based on flange draw-in samples and the feedback system stabilises the process by adjusting the blank-holder and cavity pressure during the punch stroke. The main disadvantage; dependent on accurate and robust draw-in samples as a sensor fallout will result in process instability.

- **Feedback and ILC:** The first part produced is identical to the one produced by the feedback scheme, the following parts will gradually update the process parameters according the process history i.e. the blank-holder and pressure profiles are updated before the production of the next part. Also this algorithm is depending on accurate and robust draw-in samples.

- **ILC (part to part update):** The process parameters are constant during the punch stroke - this limit the flexibility. However, the flange geometry is measured post process using e.g. a laser scanner or image processing technologies.

The selection of control schemes/algorithms are a compromise between the equipment at hand (which process parameters can be adjusted and at which speed), production rate, which sensor technology is available etc. Depending on the physical constraints different option are available, offering different levels of control and reaction speed. Taking into account the present robustness of draw-in sensors, post processing flange geometry seems to be the most promising of the three algorithms presented in this paper.

Acknowledgement

The author would like to thank the following private foundation for contributing to the research; P.A. Fiskers fond, Det Obelske Familiefond, Henry og Mary Skov, Tranes Fond, Ole Kirk's fond and Fabrikant Mads Clausens Fond.

References

[1] B Endelt. Design strategy for optimal iterative learning control applied on a deep drawing process. International Journal of Advanced Manufacturing Technology, 88(1):3–18, 2017.

[2] B. Endelt. Designing an iterative learning control algorithm based on process history - using limited post- process geometrical information. In Proceedings of the IDDRG 2017 Conference, 2017.

[3] B. Endelt and J. Danckert. Iterative learning and feedback control applied on a deep drawing process. International Journal of Material Forming, 3(SUPPL. 1):25–28, 2010.

[4] B. Endelt and W. Volk. Designing an iterative learning control algorithm based on process history - using limited post- process geometrical information. In Proceedings of the IDDRG 2013 Conference, Best in Class Stamping, 2013. submitted for presentation at the IDDRG 2013 Conference.

[5] Benny Endelt, Søren Tommerup, and Joachim Danckert. A novel feedback control system - controlling the material flow in deep drawing using distributed blank-holder force. Journal of Materials Processing Technology, 213(1):36 – 50, 2013.

[6] Jörg Heingärtner, Anja Neumann, Dirk Hortig, Yasar Rencki, and Pavel Hora. Acquisition of material properties in production for sheet metal forming processes. In AIP Conference Proceedings, volume 1567, pages 671–674. AIP, 2013.

[7] Yongseob Lim, Ravinder Venugopal, and A. Galip Ulsoy***. Advances in the control of sheet metal forming. In Proceedings of the 17th World Congress The International Federation of Automatic Control, 2008.

[8] Sy-Wei Lo and Tsu-Chang Yang. Closed-loop control of the blank holding force in sheet metal forming with a new embedded-type displacement sensor. The International Journal of Advanced Manufacturing Technology, 24(7-8):553–559, 2004.

[9] James A. Polyblank, Julian M. Allwood, and Stephen R. Duncan. Closed-loop control of product properties in metal forming: A review and prospectus. Journal of Materials Processing Technology, 214(11):2333 – 2348, 2014.

[10] K. Siegert, M. Ziegler, and S. Wagner. Closed loop control of the friction force. deep drawing process. Journal of Materials Processing Technology, 71(1):126–133, 1997.